SYNCHROTRON X-RAY DIFFRACTION ANALYSIS OF METEORITES IN THIN SECTION: PRELIMINARY RESULTS. A.H. Treiman[1], A. Lanzirotti[2], D. Xirouchakis[3] [1]Lunar & Planetary Institute, 3600 Bay Area Boulevard, Houston TX 77058 <treiman@lpi.usra.edu>, [2] Consortium for Advanced Radiation Sources, University of Chicago at Brookhaven National Laboratory, Upton NY 11973 <lanzirotti@bnl.gov>. GEOTERRA Geotechnical Consultants, Athens, Greece. <geoterra@otenet.gr>.

X-ray diffraction is the pre-eminent technique for mineral identification and structure determination [1,2], but is difficult to apply to grains in thin section, the standard meteorite preparation. Bright focused X-ray beams from synchrotrons have been used extensively in mineralogy [3,4] and have been applied to extraterrestrial particles [5]. The intensity and small spot size achievable in synchrotron X-ray beams makes them useful for study of materials in thin sections [6]. Here, we describe synchrotron X-ray diffraction (SXRD) in thin section as done at the National Synchrotron Light Source, and cite examples of its value for studies of meteorites in thin section.

Samples and Methods: The Serra de Magé meteorite is a eucrite (basalt); two thin sections of it contain a thin veinlet of a silica mineral [7]. The nakhlite meteorites are augite-rich basaltic rocks from Mars. They contain pre-terrestrial, Martian, clay-rich alterations material, iddingsite, which we examined in thin sections of Lafayette [8] and Y000749 [9,10].

Synchrotron X-ray micro-diffraction (SXRD) analyses were obtained with the hard X-ray microprobe, X26A, National Synchrotron Light Source, Brookhaven National Laboratory [11]. Synchrotron X-ray emissions from the X26A bending magnet are first collimated to 350 µm x 350 µm, monochromated (here, to 0.72084Å to coincide with MoKα X-rays), and focused to 10-µm diameter with Rh coated Kirckpatrick-Baez mirrors (X-ray flux declines between electron injections into the NSLS X-ring). The thin section is held at a fixed orientation, tilted 45° to the X-ray beam axis, so the beam impinges onto the thin section in an ellipse of ~ 10 x 15 µm. Diffracted X-rays pass through the sample (i.e. transmission mode) to the detector, a Bruker SMART 1500 CCD camera with a 4:1 fiber optic taper, in high-resolution mode at 1024x1024 pixels (96 µm pixel size). The camera was located so the X-ray beam center (undiffracted X-rays) was just off of the CCD array; camera-sample distance is adjustable. A diffraction pattern of powdered corundum (α-Al_2O_3, NIST SRM 674a) dispersed on Mylar was modeled with FIT2D [12] for best fit values of camera-sample distance, camera tilt and rotation, and location of beam center on the camera plane. Diffraction images for unknowns were calibrated with these parameters using FIT2D, and then integrated in annuli around the beam center to yield plots of diffracted intensity vs. d-spacing.

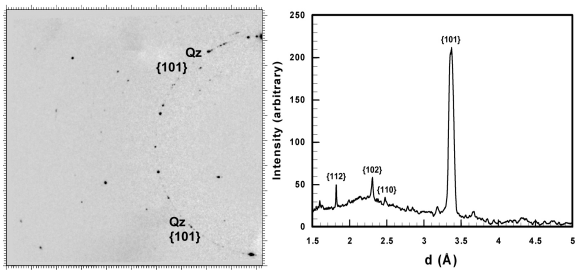

Figure 1. SXRD image and integrated intensity scan of an area in the quartz veinlet in the Serra de Magé eucrite [7]. Diffuse scattering (glass) background subtracted. Peaks are indexed for α-quartz.

In SXRD analysis, samples are not subjected to high vacuum, nor to heat. We observed no changes in samples, glass, or mounting adhesives (epoxy).

Results: SXRD analyses of materials in thin section show strong diffuse scattering from the thin-section glass around the undiffracted beam. Diffractions from the thin section material are superimposed on this diffuse background. If the sample volume illuminated by the incident beam consists of many small crystals, SXRD images show circles of diffractions (a Debye-Scherrer pattern; Fig. 1). Most single crystals are not at a diffracting orientation and show only diffuse scattering. Single crystals at diffracting conditions show portions of reciprocal lattice nets – lines or grids of diffracted beams.

Glass. Figure 2 shows SXRD results for thin section glasses. Fused silica glass shows a narrow diffraction maximum at ~4.3 Å, and an inflection at ~8.6 Å. Borosilicate glass shows a broader maximum at 3.86 Å with shoulders at ~3.7 and ~3.4 Å. Spectra like these form the background on which are superposed diffrac-

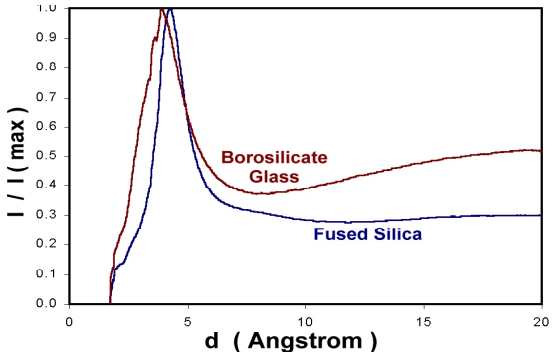

Figure 2. SXRD intensity scans for thin section glasses, relative to maximum intensity in a scan.

tions from the section materials.

Meteorite Materials. SXRD of material in thin section was first reported, to determine the mineralogy of fine-grained symplectite the Martian meteorite Los Angeles [13]. {An environmental application was reported nearly simultaneously [6].}

SXRD was crucial in interpreting a silica veinlet in the Serra de Magé cumulate eucrite meteorite, inferred to be from the asteroid 4 Vesta [7]. Optical and electron microprobe chemical analyses showed that the veinlet was of silica, SiO_2. Silica occurs in several different crystal structures, which can form in different environments. Tridymite-bearing veins in other eucrites are late magmatic [14], while quartz veins typically form from hydrothermal water. The Serra de Magé veinlets are quartz [7].

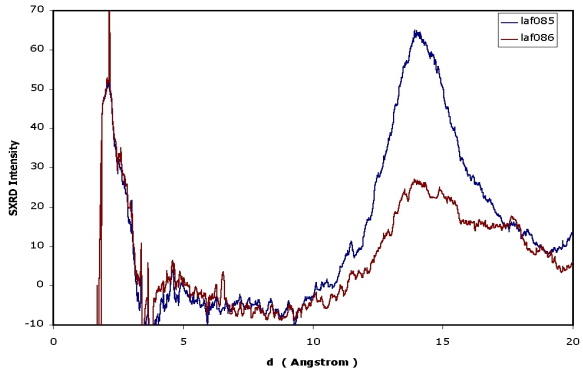

Figure 3. Background-subtracted SXRD scans for adjacent smectite grains in the Lafayette nakhlite [8]. Peak at ~3 Å is an artifact of background subtraction. The only obvious difference between the grains is their orientation, with laf085 closer to the {001} diffracting condition. The position and breadth of the diffraction maximum is consistent with a layer-disordered smectite.

The nakhlite Martian meteorites contain veinlets and patches of "iddingsite," fine-grained smectite rich material that formed on Mars [8,15,16]. The mineralogy of this "iddingsite" is important for understanding groundwater on Mars. Smectite in the nakhlite Lafayette forms grains to ~100 µm across, few of which are oriented for diffraction from the basal {001} lattice planes (Fig. 3). Grains in that diffraction orientation show a broad peak centered at ~14 Å (Fig. 3) consistent with smectite with significant layer disorder and/or interlayer substituents [17]. Iddingsite in Y000749 [9,10] is nearly amorphous to X-rays (Fig. 4). Rusty-colored areas of the iddingsite show a weak broad diffraction centered at ~14 Å, characteristic (as above) with disordered smectite. Red areas in the iddingsite show nearly no ~14 Å diffraction, but shows a strong peak at 2.56 Å, suggesting an iron oxyhydroxide (e.g., lepidocrocite or feroxyhyte).

Acknowledgments. Thin sections were loaned by the American Museum of Natural History, the Smithsonian Mu-

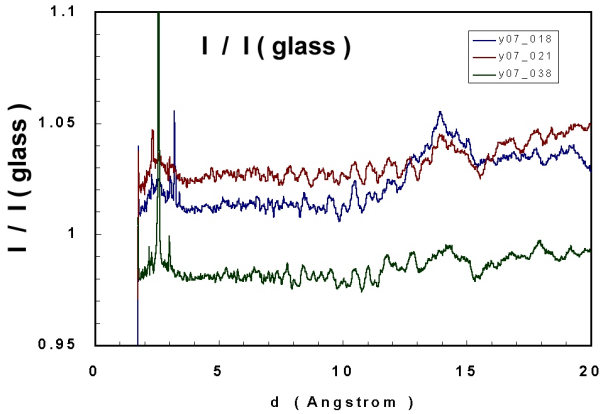

Figure 4. SXRD intensity scans for iddingsite in Y000749 [9,10], divided by intensity of thin section glass. Peak at ~14Å represents layer-disordered smectite, absent in area 038. Its strong peak at 2.56 Å may represent an Fe oxy-

seum of Natural History, the University of New Mexico Institute of Meteoritics, and the NIPR (Japan). Treiman is supported in part by NASA grants NAG5-8270 and NAG5-12184. Micro-SXRD studies at NSLS beam line X26A are supported by DOE grant DOEFG0292ER14244 to S. Sutton, M. Rivers, and A. Lanzirotti (CARS/U. Chicago). Research carried out at the National Synchrotron Light Source, Brookhaven National Laboratory, which is supported by the U.S. Department of Energy, Division of Materials Sciences and Division of Chemical Sciences, under Contract No. DE-AC02-98CH10886.

References: [1] Azaroff L. (1968) *The Powder Method*, J. Wiley. [2] Post J.E. and Bish D.L. (1989) p 277 in *Modern Powder Diffraction* (eds. D.L. Bish & J.E. Post), *Reviews In Mineralogy* 20, Min. Soc. Amer. [3] Brown G.E.Jr. & Sturchio N.C. (2002) Ch. 1 in *Applications Of Synchrotron Radiation In Low-Temperature Geochemistry And Environmental Science* (eds. P.A. Fenter et al.). Reviews in Mineralogy and Geochemistry 49, Min. Soc. Amer. [4] Manceau A. et al. (2002) Ch. 7 in *Applications Of Synchrotron Radiation In Low-Temperature Geochemistry And Environmental Science* (eds. P.A. Fenter et al.). Reviews in Mineralogy and Geochemistry v. 49, Min. Soc. Amer. [5] Flynn G.J. et al. (2000) *Lunar Planet. Sci.* XXXI, 1772. [6] Manceau A. et al. (2002) *Amer. Mineral.* **87**, 1494. [7] Treiman A.H.et al. (2004) *Earth Planet. Sci. Lett.*, in press. [8] Treiman A.H. et al. (1993) *Meteoritics* 28, 86. [9] Treiman A.H. & Goodrich C.A. (2002) *NIPR Symp. Antarctic Meteorites*, **XXVII**, 166. [10] Imae N. et al. (2003) *Antarctic Meteorite Res. (NIPR)* **16**, 13. [11] Lanzirotti A. & Sutton S. (2002) *Hard X-Ray Microprobe.* Brookhaven National Lab. website. [12] Hammersley A.P. (1998) *FIT2D V10.3 Reference Manual V4.0.* European Synchrotron Research Facility, Paper ESRF98 HA01T. website. [13] Xirouchakis D. et al. (2002) *Geochim. Cosmochim. Acta* 66, 1867. [14] Mittlefehldt D.W. & Lee M.T. (2001) *Meteorit. Planet. Sci.* 36, A136. [15] Bunch T.E. & Reid A.M. (1975) *Meteoritics* **10**, 303. [16] Gooding J.L. et al. (1991) *Meteoritics* 26, 135. [17] Carroll D. (1970) *Clay Minerals: A Guide to Their X-ray Identification*. Geol. Soc. Amer. Spec. Pub. 126.